White matter alterations of the corticospinal tract in adults born very preterm and/or with very low birth weight

Short title: Corticospinal tract in adults born preterm

Jurcoane Alina[1,2,3,4,#], Daamen Marcel[1,3], Scheef Lukas[1], Bäuml Josef G[5,6], Meng Chun[5,6], Wohlschläger Afra M[5,6], Sorg Christian[5,6,7], Busch Barbara[3], Baumann Nicole[8], Wolke Dieter[8,9], Bartmann Peter[3], Hattingen Elke[2*], Boecker Henning[1*]

[1] Functional Neuroimaging Group, Department of Radiology, University Hospital Bonn, Bonn, Germany

[2] Section of Neuroradiology, Department of Radiology, University Hospital Bonn, Bonn, Germany

[3] Department of Neonatology, University Hospital Bonn, Bonn, Germany

[4] Center for Individual Development and Adaptive Education of Children at Risk, Frankfurt am Main, Germany

[5] Department of Neuroradiology, Klinikum rechts der Isar, München, Germany

[6] TUM-NIC Neuroimaging Center, Technische Universität München, München, Germany

[7] Department of Psychiatry, Klinikum rechts der Isar, München, Germany

[8] Department of Psychology, University of Warwick, Coventry, UK

[9] Warwick Medical School, University of Warwick, Coventry, UK

* shared authorship HE and BH

Corresponding Author

Alina Jurcoane

Section of Neuroradiology

Department of Radiology

University Hospital Bonn

Sigmund-Freud-Str. 25

53105 Bonn

Tel 0049-0228287-16696

Fax 0049-0228287-14321

Email alina.jurcoane@ukb.uni-bonn.de

Keywords: preterm birth, corticospinal tract, white matter, diffusion tensor imaging

Abstract

White matter (WM) injury, either visible on conventional magnetic resonance images (MRI) or measurable by diffusion tensor imaging (DTI), is frequent in preterm born individuals and often affects the corticospinal tract (CST). The relation between visible and invisible white mater alterations in the reconstructed CST of preterm subjects has so far been studied in infants, children and up to adolescence.

Therefore, we probabilistically tracked the CST in 53 term-born and 56 very preterm and/or low birth weight (VP/VLBW, < 32 weeks of gestation and/or birth weight < 1500g) adults (mean age 26 years) and compared their DTI parameters (axial, radial, mean diffusivity – AD, RD, MD, fractional anisotropy - FA) in the whole CST and slice-wise along the CST. Additionally, we used the automatic, tract-based-spatial-statistics (TBSS) as an alternative to tractography. We compared control and VP/VLBW and subgroups with and without CST WM lesions visible on conventional MRI.

Compared to controls, VP/VLBW subjects had significantly higher diffusivity (AD, RD, MD) in the whole CST, slice-wise along the CST, and in multiple regions along the TBSS skeleton. VP/VLBW subjects also had significantly lower (TBSS) and higher (tractography) FA in regions along the CST, but no different mean FA in the tracked CST as a whole. Diffusion changes were weaker, but remained significant for both, tractography and TBSS, when excluding subjects with visible CST lesions.

Chronic CST injury persists in VP/VLBW adults even in the absence of visible WM lesions, indicating long-term structural WM changes induced by premature birth.

Introduction

Preterm birth (before 37 weeks of gestation) has a lifelong impact on neurodevelopment [Mwaniki et al., 2012]. Cognitive, motor and sensory deficits persist into adulthood and morbidity is inversely related to gestational age at birth [Saigal and Doyle, 2008] and/or to birth weight. As such, very preterm (VP, birth before 32 weeks of gestation) and/or very low birth weight (VLBW, <1500 g) individuals have an especially high risk of morbidity [Lawrence et al., 2014] and although some of the deficits may improve [Marlow et al., 1993], most studies report a persistence of functional impairments into young adulthood [Allin et al., 2006; Sripada et al., 2015].

The functional deficits in preterm born individuals are associated with cerebral white matter (WM) and grey matter (GM) abnormalities, coined as "encephalopathy of prematurity" [Volpe, 2009a; Volpe, 2009b]. The dominant pathology is white matter injury which occurs in 50% or more of VP/VLBW [Pandit et al., 2013; Volpe, 2009a; Volpe, 2009b] and is a combination of focal deep periventricular lesions visible on conventional MRI and diffuse injuries uncovered only by advanced imaging techniques such as diffusion weighted imaging and its application, diffusion tensor imaging (DTI). DTI characterizes the size and directional preference of tissue water diffusion and provides objective measures that reflect tissue microstructure [Le Bihan et al., 2001]. DTI parameters such as axial, radial and mean diffusivity (AD, RD and MD, respectively) as well as fractional anisotropy (FA) are usually altered in preterm born subjects compared to controls (for a review see [Pandit et al., 2013]). Such white matter alterations have been reported in infancy (reviewed in [Pannek et al., 2014]), childhood [de Kieviet et al., 2014], adolescence (reviewed in [Ment et al., 2009]) and in young adulthood [Allin et al., 2011; Eikenes et al., 2011]. In general, various degrees of increased diffusivity and decreased anisotropy are observed, although not all studies could replicate these findings [Li et al., 2014]. The majority of studies found a consistent increase of diffusivity - mean or radial - but the anisotropy may not always be decreased. A recent meta-analysis of DTI studies in infants, children and adolescents [Li et al., 2014] found decreased FA in multiple regions including the corpus callosum, superior longitudinal fasciculus, external capsule, posterior thalamic radiation and cingulum, but the same meta-analysis also identified regions in the corona radiata with increased fractional anisotropy.

White matter injury frequently affects the motor pathways and is strongly associated with motor impairments [Scheck et al., 2012; Staudt et al., 2003], ranging from minor motor dysfunction to most severe motor disability, cerebral palsy. Together with other impairments, motor deficits have detrimental effects on long-term functional outcomes of preterm born individuals [Anderson, 2014; Bracewell and Marlow, 2002]. Therefore, characterizing structural alterations along the corticospinal tract (CST) is of particular clinical neuroscientific interest. So far, white matter alterations within the

CST have been studied in infants and children [Bassi et al., 2011; Estep et al., 2014], as well as adolescents [Groeschel et al., 2014], but beyond reports of widespread white matter changes found in whole brain analyses in adults [Allin et al., 2011; Eikenes et al., 2011], no study focussed on the reconstructed CST in adults. Thus, we aimed to assess group differences in WM changes of the CST between VP/VLBW and term born adults by DTI and to evaluate the impact of visible lesions on DTI parameters in and along the CST.

Methods

Subjects

Study participants were recruited from the prospective Bavarian Longitudinal Study (BLS), a geographically defined whole-population sample of VP/VLBW and term-born individuals who were followed up from birth into young adulthood [Riegel et al., 1995; Wolke and Meyer, 1999]. Following completion of adult behavioral assessments eligible participants were invited for a later MRI examination (including the DTI protocol). Before entering this MRI substudy, each participant was carefully screened for MR-related contraindications (e.g., pregnancy, claustrophobia, or ferromagnetic or electrical implants). MRI examinations were conducted either at the Department of Radiology of the University Hospital Bonn, Germany, or at the Department of Neuroradiology, Technische Universität München, Germany. The study complies with the Code of Ethics of the World Medical Association (Declaration of Helsinki), local ethics committees at each of the two sites approved the study, and all participants gave informed consent prior to examination.

VP/VLBW participants were recruited from the whole population of at-risk infants born alive in Southern Bavaria, Germany, between January 1985 and March 1986 who required admission to one of the 16 children's hospitals within the first 10 days of life (N=7,505; 10.6% of all live births)[Wolke and Meyer, 1999]. Of this basic cohort, 682 children were born VP/VLBW. 172 died during initial hospitalization and 12 died between discharge and 26 years assessments. Seven parents did not give consent to participate, while 43 parents and their children were non-German speakers and had to be excluded as cognitive assessments could not be administered. No contact information was available for 37 VP/VLBW adults. Of the eligible 411 VP/VLBW survivors, 260 (63.3%) participated in 26-years follow-up assessments[Daamen et al., 2014], with 104 (25.3%) undergoing the additional MRI examination.

A comparison sample of term-born born infants (GA >36 weeks) was recruited from normal postnatal wards in the same obstetric hospitals as VP/VLBW participants. Of the initial 916 control children alive at 6 years, 350 were randomly selected as term controls, using the stratification variables sex

and family socioeconomic status (SES) to be comparable with the VP/VLBW cohort at age 6 years 3 months. Of these, 308 were eligible for 26 year follow-up assessments, with 229 (74.4%) participating in the psychological assessments, and 110 (35.6%) completing the additional MRI examination.

From this MRI sample, 109 subjects, 53 term born and 56 VP/VLBW, were selected (see Table 1), following exclusion of datasets with moderate-to-severe artifacts (n=85) (see detailed description under Methods: Quality Check) and exclusion of subjects without a complete DTI measurement (n=20).

Clinical measures. Birth related parameters such as gestational age, birth weight and a 21 items neonatal optimality score [Prechtl, 1967; Wolke and Meyer, 1999], which measured the extent of neonatal clinical complications, were available from the neonatal assessments (see [Gutbrod et al., 2000]). Tests of motor function were available for age 6 and 8 years: the Beery Developmental Test of Visual-Motor Integration[Beery KE, 1982] and the test of motor impairment[Stott et al., 1984]. At age 26 several cognitive [Eryigit Madzwamuse et al., 2014] but no motor tests were available.

Image acquisition

The MRI measurements were performed in Bonn (n=48) at the Department of Radiology, University Hospital Bonn, Germany, and in Munich (n=61) at the Department of Neuroradiology, Technische Universität München, Germany (see Table 1). We used 3 Tesla scanners (Table 1) with a 8-channel head coil for all measurements. Due to scanner upgrades, both sites had to shift from 3T Achieva TX to complementary 3T Ingenia systems, which necessitated slight adaptions of scan sequence parameters. The possible impact of different scanners on the study results was statistically tested and is reported.

Diffusion-weighted images for DTI were acquired with a single-shot spin-echo echo-planar imaging sequence (repetition time TR 20163 ms, echo time TE 47 ms, flip angle 90°, 75 slices, matrix 112x112, voxel size 2x2x2 mm), with b-values of 0 and 1000 s/mm^2 and a gradient scheme with 32 non-collinear diffusion directions.

Whole brain, high-resolution T1-weighted (T1w) images were obtained with a 3D- Turbo Field Echo sequence (TR 7.7 ms, TE 3.93 ms, flip angle 15°, 180 slices, matrix 256x256, voxel size 1x1x1 mm, parallel acquisition with SENSE 2), and were used for coregistration purposes and identification of gross anatomical changes.

For identification of visible white matter changes we recorded 3D fluid-attenuation inversion recovery (FLAIR) images (TR 4800ms, inversion time TI 1600 ms, SENSE 5) and T2-w images (3D turbo

spin echo with flip angle sweep 35°, TR 2500 ms, flip angle 90°, SENSE 4). Both FLAIR and T2-w images were acquired with fat suppression, 360 overcontiguous slices, matrix 512x512, acquired voxel size 1x1x1 mm, reconstructed voxel size 0.5x0.5x0.5mm.

Data analysis

The software package FSL v5.0 (FMRIB Software Library, Oxford, UK - http://fsl.fmrib.ox.ac.uk/fsl/fslwiki/) [Jenkinson et al., 2012] was used to analyze CST white matter integrity, applying two methods: probabilistic tractography and tract-based spatial statistics (TBSS, [Smith et al., 2006]).

Preprocessing. We first corrected the raw DTI images for motion and eddy current effects by linear registration to the first b0 volume. Then we skull-stripped the result with the Brain Extraction Tool (BET) [Smith, 2002]. Finally we fitted the tensor model with DTIFIT (FSL) to obtain the diffusion maps: FA, AD (λ1), RD (λ2 + λ3) / 2) and MD (λ1 + λ2 + λ3) / 3).

Quality check. Apart from careful visual inspection of raw data, we also used the fitting residuals (the sum-of-squared error maps generated by DTIFIT) to identify data corrupted by artifacts. In case of poor fitting due to motion artifacts (signal loss), we either discarded the whole dataset or, if less than four volumes (gradients) were corrupted, we discarded those volumes [Heemskerk et al., 2013] and refitted the remaining data. Poor fitting also occurred due to other, non-correctable artifacts such as projection of skull-fat onto the brain (ghosting) [Tournier et al., 2011] due to insufficient fat suppression [Sarlls et al., 2011] and/or unfortunate head positioning. In these cases, we carefully rated the artifact intensity by a four-point visual rating scale - no/minimal artifact (n=72), weak (n=37), medium (n=23) or strong artifact (n=62). For this study, out of the pool of n=194 full DTI datasets initially available, we excluded datasets rated as medium or strong artifact (n=85).

Probabilistic tractography. We used probabilistic tractography [Behrens et al., 2003] to reconstruct the CST in each hemisphere and subject from seed to target regions defined in the standard space of the Montreal Neurological Institute (MNI152) template [Giorgio et al., 2010]. The distribution of diffusion directions at each voxel was reconstructed with BEDPOSTX (FSL) with two crossing fibers modeled per voxel. The probabilistic tractography algorithm repeatedly sampled up to 5000 of these directions and generated a probabilistic streamline between seed and target. We used a seed in the cerebral peduncle at z=-22, a target in the precentral gyrus at z=56 and termination masks below the seed and above the target regions. To remove spurious connections in the final CST path we only selected those voxels through which at least 20 samples passed [Giorgio et al., 2010]. This method has been shown to robustly reconstruct the CST even in subjects with distorted anatomical features such as enlarged ventricles [Jurcoane et al., 2014]. The FA, AD, MD and RD parameters in the left and

right CST were then extracted and compared between the VP/VLBW and control groups, once with and again without white-matter lesions. Furthermore, we also generated a slice-wise tract profile containing the DTI parameters along the superior-inferior axis of the CST and identified the levels that were significantly different between the groups.

Tract-based-spatial-statistics (TBSS). We used TBSS as an alternative, supportive method for our main probabilistic tractographic approach. TBSS is a voxelwise statistical analysis of diffusion data, which creates a thinned, skeletonized mean FA image (of FA values above 0.2) from all subjects' FA data non-linearly aligned to the standard MNI152 brain. This skeletonized FA image represents the centers of all tracts common to all the subjects onto which each subject's FA, AD, MD or RD data is projected and statistically compared. We used “randomise” (FSL) with 5000 permutations, and multiple comparisons correction by means of threshold-free cluster enhancement (TFCE, [Smith and Nichols, 2009]) to compute the group differences between the VP/VLBW and the control group within the skeleton masked with the average-CST (from probabilistic tractography).

Visible lesions in the white matter were identified on the FLAIR and T2-weighted images by an experienced neuroradiologist (EH), who noted whether lesions were present and if yes, whether they were located along the CST. We then used this information to analyze the DTI data of the CST in subjects with and without lesions along the tract. Volumes of the lateral ventricles (enlargement) and corpus callosum (thinning) in T1-w images were visually evaluated and quantified based on T1-w image segmentation (see supplemental Figure). Values beyond one standard deviation from the mean volume of control subjects are reported.

Statistics

Statistical analysis was performed with FSL [Jenkinson et al., 2012] and with R Statistics package (version 3.2.1) (http://www.R-project.org/, [R Core Team, 2014]).

We used independent samples t-tests to compare VP/VLBW and controls. For categorical variables, we used a chi-squared test. We assessed the correlation between DTI parameters in the CST and birth-related variables or motor scores with Pearson's correlation coefficient. Differences between subgroups with and subgroups without white matter lesions were explored with the analysis of variance (ANOVA). We considered a p value < 0.05 as statistically significant and we used a Bonferroni correction for multiple comparisons for the tests along the CST profile.

Results

The corticospinal tract was successfully reconstructed in every single subject.

Whole sample analysis

Axial, radial and mean diffusivity were all higher in VP/VLBW than in controls (Table 2 and Figure 1), both for the whole CST (Figure 1a) and along the tract in the corona radiata near the lateral ventricles and the centrum semiovale, as well as in selected portions of the capsula interna and the brain stem (Figure 1b). Fractional anisotropy was not different between the groups for the whole tract but VP/VLBW had higher FA in the CST at the level of the corona radiata.

TBSS (Figure 2) also revealed higher diffusivities (AD, RD, MD) in the CST of the VP/VLBW subjects compared to controls and the location of these differences followed the pattern found in the tractography analysis. TBSS found no regions of higher FA but uncovered regions (in the centrum semiovale and the brain stem) of lower fractional anisotropy in the CST of the VP/VLBW subjects.

In the VP/VLBW group, 28 (50%) subjects had no visible WM hyperintensities on the MR FLAIR or T2 images, 18 (32%) had WM hyperintensities affecting the CST and 10 (18%) had hyperintensities in the WM outside the CST or in the periventricular regions. In the control group, 42 subjects (79%) had normal MRIs, three (6%) had hyperintensities in the CST and eight (15%) subjects had hyperintensities outside the CST (see Figure 3). On the T1w conventional MRI images, the visual inspection as well as the volume quantification (see supplemental Figure) showed that half of VP/VLBW had enlarged ventricles with undulating ventricular borders and callosal thinning, while only one tenth of controls had enlarged ventricles with undulating ventricular borders and less than one fifth of controls had callosal thinning.

We found no significant correlations between diffusion parameters (FA, AD, RD, MD) and birth related variables (gestational age, birth weight and optimality score), or motor scores at age 8.

Subgroup analysis

A rerun of the tractography and TBSS analyses in subgroups without visible WM hyperintensities in the CST showed weaker, but still significant effects, similar to the whole sample analysis (Table 3). Post hoc comparisons using the Tukey HSD test indicated that mean AD and MD in the CST were significantly higher in both, VP/VLBW without WM lesions and VP/VLBW with WM lesions, compared to controls (Table 3, contrasts 1-3 and 1-4). VP/VLBW subjects with lesions in the CST tended to have higher AD ($p=0.07$) than VP/VLBW subjects without CST lesions (Table 3, contrast 2-4).

Exploratory analyses of confounding factors

Right-left asymmetry - in both VP/VLBW and controls, the diffusivity values (AD, RD, MD) were significantly higher in the left hemisphere (VP/VLBW $F(1,110)>6$, $p<0.05$; controls $F(1,104)>6$, $p<0.05$) whereas the FA did not differ between the two sides. However, the main group effect

(VP/VLBW>controls) was significant in each hemisphere. Table 2 and Figure 1 therefore depict the comparison of DTI values in the whole CST (right and left averaged). TBSS analysis of right-left symmetry also confirmed the higher diffusivities in the left hemisphere in both the VP/VLBW and control subjects.

Scanner effects. During the acquisition period of almost three years (beginning of 2011 until end of 2013), both MRI sites shifted from a Philips Achieva 3T to a Philips Ingenia 3T scanner for reasons that were independent of the present study. As a result, the DTI data in this study arise from four different scanners - albeit, two thirds of the data do come from two scanners (see Table 1). Nevertheless, we could replicate the main group effects reported above (diffusivity VP/VLBW>controls) in each of the two scanners with most subjects and therefore we report here the pooled results of all subjects and scanners.

Artifacts. The analysis (tractography and TBSS) of a subset of data (n=72, 36 VP/VLBW, 36 controls) free from any kind of artifacts delivered the same effects as of those presented here.

Discussion

DTI revealed significant WM alterations along the CST in adult VP/VLBW subjects compared to term born individuals. These alterations were significant regardless of the presence or absence of CST white matter lesions, which were visible in FLAIR and T2-w images, and suggest diffuse CST injury (not visible on conventional MRI) that persists into adulthood.

In line with previous findings [Pandit et al., 2013; Volpe, 2009a; Volpe, 2009b] about half of the VP/VLBW subjects had various degrees of brain abnormalities visible on conventional MRI (enlarged ventricles, thinning of the corpus callosum or white matter lesions).

Our study extends previous findings of altered WM microstructure in VP/VLBW subjects. There are reports on widespread WM disturbances in younger adults who were born preterm [Allin et al., 2011; Eikenes et al., 2011]. These changes affect the corpus callosum, the superior longitudinal fasciculi, the corona radiata [Allin et al., 2011] and also the CST [Eikenes et al., 2011; Groeschel et al., 2014]. Higher MD and lower FA are the usual findings but higher FA is not uncommon (for a meta-analysis see [Li et al., 2014]). However, the diffusion properties and their relation to visible WM lesions in the CST of preterm born subjects have so far been only reported in infants [Bassi et al., 2011], children [Estep et al., 2014] and adolescents [Groeschel et al., 2014] but not in adults. Previous studies demonstrated that white matter pathology visible on conventional MRI leads to increased diffusivity, which is suggestive of increased water content in the affected white matter tracts [Counsell et al., 2003]. We found such increased diffusivity even in the absence of visible WM lesions suggesting even more subtle white matter alterations in the CST of VP/VLBW. These

alterations may be related to the "encephalopathy of prematurity" [Volpe, 2009a] since the CST is an early myelinating tract running in the periventricular area through part of its course and may be particularly vulnerable to injury [Estep et al., 2014]. In infants, Bassi et al. [Bassi et al., 2011] also found such diffuse injury extending beyond the lesion boundaries but they limited their observation to FA. Estep et al [Estep et al., 2014] demonstrated higher diffusivities in the right CST of very preterm children with moderate-to-severe visible WM alterations compared to very preterm children without WM alterations. They interpreted these findings as reflecting disrupted fiber tracts, reduced myelin, and/or lower axonal density.

Compared with controls adolescents born preterm have significantly altered diffusion parameters at several levels along the cortico-spinal, thalamo-cortical and transcallosal pathways [Groeschel et al., 2014]. A crucial aspect of these findings is that while MD was consistently increased along the CST, FA was decreased in single fiber regions (i.e. in the internal capsule) and increased in crossing fiber regions (i.e. in the centrum semiovale). Our results confirm these findings, albeit, only in part: our TBSS analysis showed decreased FA in the capsula interna but also in the centrum semiovale. While we found no regions of increased FA with TBSS, these were uncovered by the probabilistic tractography, which showed higher FA in VP/VLBW in the corona radiata near the lateral ventricles. Corroborating our results from the two modalities (TBSS and tractography) may explain why we found no significant FA difference between VP/VLBW and controls in the CST as a whole: If parts of the CST exhibit higher FA and parts exhibit lower FA, it is unlikely that the average of these FA values are significantly different.

Supporting our findings Groeschel et al [Groeschel et al., 2014] found that alterations in the CST in adolescents were weaker but, at least for FA, were maintained when analyzing only the subjects without visible WM injury.

Increased overall diffusivity may actually suggest chronic injury [Aung et al., 2013] and elevated water content [Counsell et al., 2003]. Reduced anisotropy is usually associated with less myelin and/or lower axonal density [Estep et al., 2014; Song et al., 2002] but there are few explanations for increased FA. One explanation discussed by Groeschel et al [Groeschel et al., 2014] is related to crossing fibers, where selective FA decreases in one of the crossing fibers may result in apparent FA increases in the other fiber. More precisely, FA along the CST could be artificially induced by a decrease in FA in a perpendicular tract crossing in the same voxel. Another explanation would be a mechanical stress of fibers running near the lateral ventricles. We previously could show that ventricular enlargement causes an increase of FA values along the CST [Jurcoane et al., 2014]. Our finding [Jurcoane et al., 2014] was in patients with normal pressure hydrocephalus but adults born

preterm also have a significant enlargement of their ventricles compared to adults born term [Nosarti et al., 2002].

Currently it is still not clear how big the impact of structural CST abnormalities upon motor function may be. A recent review of studies examining cerebral palsy concluded that decreased FA and increased MD within descending motor tracts, particularly the CST, reflect tract integrity and, hence, correlate with the clinical severity of cerebral palsy [Scheck et al., 2012]. However, it would be hard to draw such clear-cut conclusions in preterm born individuals with milder motor impairments. On one hand, tests for motor function also engage cognitive abilities and disentangling the two is not trivial. On the other hand, there is a high variability in used methodologies between studies, which sometimes leads to contradictory findings. Nevertheless, some studies [van Kooij et al., 2012; Skranes et al., 2007] found associations between gross and/or fine motor functions and diffusion parameters: motor proficiency correlated positively with anisotropy and negatively with diffusivity, not only in the CST and the posterior limb of the internal capsule but also in the corpus callosum, the superior longitudinal fasciculus, fornix, cingulum and other tracts (for a review see Pandit et al [Pandit et al., 2013]). Sripada et al [Sripada et al., 2015] recently revealed that visual–motor performance in very low birth weight adults correlates positively with fractional anisotropy in several white matter bundles and these correlations are primarily driven by an increase in radial diffusivity. A limitation of our study is the absence of motor functional scores at the time of MRI, at age 26. Motor functioning tests were only available at age 8 and we found no correlation with the DTI parameters. Moreover, even if we had found such an association, the interpretability of such correlations would have been limited due to the long time gap. We plan a follow-up study of the same subjects in the next recruitment phase in which the motor function shall also be investigated and the combination with motor functional MRI may further clarify the impact of microstructural CST abnormalities on motor function.

We found a significant right-left asymmetry with higher diffusivities (AD, RD, MD) in the left hemisphere in both VP/VLBW and controls. A significant right-left asymmetry has been reported previously [Fabiano et al., 2005; Klingberg et al., 1999; Naganawa et al., 2003] but to date this phenomenon has not been properly explained. Fabiano et al [Fabiano et al., 2005] found higher diffusivity in several grey matter subcortical structures in the left hemisphere, but no right-left differences were reported in the white matter. Naganawa et al [Naganawa et al., 2003] also found higher diffusivity on the left side in a large cohort of 294 healthy subjects in several regions including in the thalamus and temporal white matter but these were not constant over age groups, gender and laterality, leading the authors to admit that they do not yet have a reasonable explanation for their findings. We did not find any asymmetries in the anisotropy of the CST but some studies [Klingberg et al., 1999] reported higher FA on the right side of the brain, which they interpreted as a physiological

finding in normal development. Estep et al [Estep et al., 2014] found higher diffusivities in the right CST of children with visible WM lesions and interpreted them in the context of developmental changes and non-dominance of the right hemisphere. Most studies, however, have not reported hemispheric asymmetries of diffusion parameters either because they did not search for it or because many studies usually collapse left and right hemispheres, potentially masking left-right differences. Another, more trivial explanation for these findings may be a scanner-related (coil inhomogeneity) left-right gradient. This could be investigated by scanning the same subjects while lying face up and face down in the scanner (or lying on their left and right side), but to our knowledge, no such systematic analysis has been performed so far. Thus, until this issue is thoroughly investigated, caution is advised in interpreting these asymmetries as pathology.

Methodical issues

We used two independent methods - tractography and TBSS - to investigate the diffusion changes in the CST of VP/VLBW adults and their relation to visible white matter lesions. TBSS is widely used in the analysis of white matter [Bassi et al., 2011; Eikenes et al., 2011] but TBSS biases analysis towards regions of high white matter anisotropy and underestimates the regional extent of any abnormalities[Bassi et al., 2011]. Probabilistic tractography does not suffer from these disadvantages; it reconstructs a complete fiber tract in indivdual subjects, irrespective of inter-subject anatomical differences or white matter quality and tracks even through regions of high uncertainty due to fiber crossings or white matter lesions. That is why we focused on probabilistic tractography and used TBSS primarily as a confirmatory analysis for our tractography findings.

We carefully quality-checked our data and excluded data with severe artifacts. However, we did include datasets (n=37) with weak artifacts resulting from insufficient fat-suppression. We chose to do this because the analysis (tractography and TBSS) of the subset of data (n=72, 36 VP/VLBW, 36 controls) free from any kind of artifacts delivered the same results as those presented here. Although our results were replicated even when including all datasets available (n=194), that is, with severe artifacts, inclusion of data severely affected by artifacts is strongly discouraged [Heemskerk et al., 2013; Sarlls et al., 2011; Tournier et al., 2011]. Until further research determines the impact of severe artifacts from insufficient fat suppression onto the resulting parameter maps, and the suitability of such data for further analysis, we chose to limit our present report to datasets without such severe artifacts.

A limitation of our study is the use of four MRI-scanners. However, all scanners had the same manufacturer and field strength (Philips 3 Tesla) and parameters of the MR-sequences were very similar. As there were no significant scanner-group interactions and main group effects were

significant in each of the two scanners with most subjects, we assume that the reported effects were not primarily driven by this limitation.

Conclusion

The diffuse perinatal WM damage in VP/VLBW-subjects even in the absence of visible WM lesions, indicates long-term structural white-matter changes induced by premature birth.

Acknowledgements

We thank Prof. Hans Schild and Prof. Claus Zimmer for enabling this study, the MR staff in Bonn and Munich for their support, Dr. Jason Martin, Dr. Kate Watkins, Dr. Saad Jbabdi and Dr. Jürgen Gieseke for insightful discussions and analysis tips, and Thomas Sattler for scripting support. Moreover, we thank all current and former Bavarian Longitudinal Study Group members who contributed to study organization, recruitment, data collection, management and analyses, including (in alphabetical order): Stephan Czeschka, Claudia Grünzinger, Julia Jäkel, Christian Koch, Diana Kurze, Sonja Perk, Andrea Schreier, Antje Strasser, Julia Trummer, and Eva van Rossum. Most importantly, we thank all our study participants for their efforts to take part in this study. This study was funded by the German Federal Ministry of Education & Science (BMBF) and by the Kommission für Klinische Forschung, Technische Universität München.

References

Allin M, Rooney M, Griffiths T, Cuddy M, Wyatt J, Rifkin L, Murray R (2006): Neurological abnormalities in young adults born preterm. J Neurol Neurosurg Psychiatry 77:495–499.

Allin MPG, Kontis D, Walshe M, Wyatt J, Barker GJ, Kanaan RAA, McGuire P, Rifkin L, Murray RM, Nosarti C (2011): White matter and cognition in adults who were born preterm. PLoS One 6:e24525.

Anderson PJ (2014): Neuropsychological outcomes of children born very preterm. Semin Fetal Neonatal Med 19:90–96. http://www.ncbi.nlm.nih.gov/pubmed/24361279.

Aung WY, Mar S, Benzinger TL (2013): Diffusion tensor MRI as a biomarker in axonal and myelin damage. Imaging Med 5:427–440.

Bassi L, Chew A, Merchant N, Ball G, Ramenghi L, Boardman J, Allsop JM, Doria V, Arichi T, Mosca F, Edwards AD, Cowan FM, Rutherford MA, Counsell SJ (2011): Diffusion tensor imaging in preterm infants with punctate white matter lesions. Pediatr Res 69:561–566. http://www.ncbi.nlm.nih.gov/pubmed/21386750.

Beery KE (1982): Revised administration, scoring, and teaching manual for the developmental test of visual–motor integration. Cleveland-Toronto: Modern Curriculum Press.

Behrens TEJ, Woolrich MW, Jenkinson M, Johansen-Berg H, Nunes RG, Clare S, Matthews PM, Brady JM, Smith SM (2003): Characterization and Propagation of Uncertainty in Diffusion-Weighted MR Imaging. Magn Reson Med 50:1077–1088.

Le Bihan D, Mangin JF, Poupon C, Clark CA, Pappata S, Molko N, Chabriat H (2001): Diffusion tensor imaging: concepts and applications. J Magn Reson Imaging 13:534–546.

Bracewell M, Marlow N (2002): Patterns of motor disability in very preterm children. Ment Retard Dev Disabil Res Rev 8:241–248.

Counsell SJ, Allsop JM, Harrison MC, Larkman DJ, Kennea NL, Kapellou O, Cowan FM, Hajnal J V, Edwards AD, Rutherford MA (2003): Diffusion-weighted imaging of the brain in preterm infants with focal and diffuse white matter abnormality. Pediatrics 112:1–7.

Daamen M, Bäuml JG, Scheef L, Sorg C, Busch B, Baumann N, Bartmann P, Wolke D, Wohlschläger A, Boecker H (2014): Working memory in preterm-born adults: Load-dependent compensatory activity of the posterior default mode network. Hum Brain Mapp 36:1121–1137. http://doi.wiley.com/10.1002/hbm.22691.

Eikenes L, Løhaugen GC, Brubakk A-M, Skranes J, Håberg AK (2011): Young adults born preterm with very low birth weight demonstrate widespread white matter alterations on brain DTI. Neuroimage 54:1774–1785.

Eryigit Madzwamuse S, Baumann N, Jaekel J, Bartmann P, Wolke D (2014): Neuro-cognitive performance of very preterm or very low birth weight adults at 26 years. J Child Psychol Psychiatry:n/a–n/a. http://doi.wiley.com/10.1111/jcpp.12358.

Estep ME, Smyser CD, Anderson PJ, Ortinau CM, Wallendorf M, Katzman CS, Doyle LW, Thompson DK, Neil JJ, Inder TE, Shimony JS (2014): Diffusion tractography and neuromotor outcome in very preterm children with white matter abnormalities. Pediatr Res 76:86–92. http://www.ncbi.nlm.nih.gov/pubmed/24713814.

Fabiano AJ, Horsfield MA, Bakshi R (2005): Interhemispheric asymmetry of brain diffusivity in normal individuals: a diffusion-weighted MR imaging study. AJNR Am J Neuroradiol 26:1089–1094.

Giorgio A, Watkins KE, Chadwick M, James S, Winmill L, Douaud G, De Stefano N, Matthews PM, Smith SM, Johansen-Berg H, James AC (2010): Longitudinal changes in grey and white matter during adolescence. Neuroimage 49:94–103.

Groeschel S, Tournier J-DD, Northam GB, Baldeweg T, Wyatt J, Vollmer B, Connelly A (2014): Identification and interpretation of microstructural abnormalities in motor pathways in adolescents born preterm. Neuroimage 87:209–219.

Gutbrod T, Wolke D, Soehne B, Ohrt B, Riegel K (2000): Effects of gestation and birth weight on the growth and development of very low birthweight small for gestational age infants: a matched group comparison. Arch Dis Child Fetal Neonatal Ed 82:F208–14.

Heemskerk AM, Leemans A, Plaisier A, Pieterman K, Lequin MH, Dudink J (2013): Acquisition guidelines and quality assessment tools for analyzing neonatal diffusion tensor MRI data. AJNR Am J Neuroradiol 34:1496–1505.

Jenkinson M, Beckmann CF, Behrens TEJ, Woolrich MW, Smith SM (2012): FSL. Neuroimage 62:782–790.

Jurcoane A, Keil F, Szelenyi A, Pfeilschifter W, Singer OC, Hattingen E (2014): Directional diffusion of corticospinal tract supports therapy decisions in idiopathic normal-pressure hydrocephalus. Neuroradiology 56:5–13.

De Kieviet JF, Heslenfeld DJ, Pouwels PJW, Lafeber HN, Vermeulen RJ, van Elburg RM, Oosterlaan J (2014): A crucial role for white matter alterations in interference control problems of very preterm children. Pediatr Res 75:731–737.

Klingberg T, Vaidya CJ, Gabrieli JD, Moseley ME, Hedehus M (1999): Myelination and organization of the frontal white matter in children: a diffusion tensor MRI study. Neuroreport 10:2817–2821.

Van Kooij BJM, de Vries LS, Ball G, van Haastert IC, Benders MJNL, Groenendaal F, Counsell SJ (2012): Neonatal tract-based spatial statistics findings and outcome in preterm infants. AJNR Am J Neuroradiol 33:188–194.

Lawrence EJJ, Walsh SF, Neilan R, Nam KWW, Giampietro V, McGuire P, Murray RMM, Nosarti C, Froudist-Walsh S, Neilan R, Nam KWW, Giampietro V, McGuire P, Murray RMM, Nosarti C (2014): Motor fMRI and cortical grey matter volume in adults born very preterm. Dev Cogn Neurosci 10C:1–9. http://www.sciencedirect.com/science/article/pii/S1878929314000425.

Li K, Sun Z, Han Y, Gao L, Yuan L, Zeng D (2014): Fractional anisotropy alterations in individuals born preterm: a diffusion tensor imaging meta-analysis. Dev Med Child Neurol.

Marlow N, Roberts L, Cooke R (1993): Outcome at 8 years for children with birth weights of 1250 g or less. Arch Dis Child 68:286–290.

Ment LR, Hirtz D, Hüppi PS (2009): Imaging biomarkers of outcome in the developing preterm brain. Lancet Neurol 8:1042–1055.

Mwaniki MK, Atieno M, Lawn JE, Newton CRJC (2012): Long-term neurodevelopmental outcomes after intrauterine and neonatal insults: a systematic review. Lancet 379:445–452.

Naganawa S, Sato K, Katagiri T, Mimura T, Ishigaki T (2003): Regional ADC values of the normal brain: differences due to age, gender, and laterality. Eur Radiol 13:6–11.

Nosarti C, Al-Asady MHS, Frangou S, Stewart AL, Rifkin L, Murray RM (2002): Adolescents who were born very preterm have decreased brain volumes. Brain 125:1616–1623.

Pandit AS, Ball G, Edwards a. D, Counsell SJ (2013): Diffusion magnetic resonance imaging in preterm brain injury. Neuroradiology 55 Suppl 2:65–95.

Pannek K, Scheck SM, Colditz PB, Boyd RN, Rose SE (2014): Magnetic resonance diffusion tractography of the preterm infant brain: a systematic review. Dev Med Child Neurol 56:113–124.

Prechtl HF (1967): Neurological sequelae of prenatal and perinatal complications. Br Med J 4:763–767.

R Core Team (2014): R: A Language and Environment for Statistical Computing. R Found Stat Comput Vienna, Austria. http://www.r-project.org/.

Riegel K, Ohrt B, Wolke D, Österlund K (1995): Die Entwicklung gef{ä}hrdet geborener Kinder bis zum f{ü}nften Lebensjahr. (The development of at-risk children until the fifth year of life. The Arvo Ylpp{ö} longitudinal study in South Bavaria and South Finland). Stuttgart Ferdinand Enke Verlag.

Saigal S, Doyle LW (2008): An overview of mortality and sequelae of preterm birth from infancy to adulthood. Lancet 371:261–269.

Sarlls JE, Pierpaoli C, Talagala SL, Luh W-MM (2011): Robust fat suppression at 3T in high-resolution diffusion-weighted single-shot echo-planar imaging of human brain. Magn Reson Med 66:1658–1665.

Scheck SM, Boyd RN, Rose SE (2012): New insights into the pathology of white matter tracts in cerebral palsy from diffusion magnetic resonance imaging: a systematic review. Dev Med Child Neurol 54:684–696.

Skranes J, Vangberg TR, Kulseng S, Indredavik MS, Evensen KAI, Martinussen M, Dale AM, Haraldseth O, Brubakk A-M (2007): Clinical findings and white matter abnormalities seen on diffusion tensor imaging in adolescents with very low birth weight. Brain 130:654–666.

Smith SM (2002): Fast robust automated brain extraction. Hum Brain Mapp 17:143–155.

Smith SM, Jenkinson M, Johansen-Berg H, Rueckert D, Nichols TE, Mackay CE, Watkins KE, Ciccarelli O, Cader MZ, Matthews PM, Behrens TEJ (2006): Tract-based spatial statistics: voxelwise analysis of multi-subject diffusion data. Neuroimage 31:1487–1505. http://dx.doi.org/10.1016/j.neuroimage.2006.02.024.

Smith SM, Nichols TE (2009): Threshold-free cluster enhancement: addressing problems of smoothing, threshold dependence and localisation in cluster inference. Neuroimage 44:83–98.

Song S-K, Sun S-W, Ramsbottom MJ, Chang C, Russell J, Cross AH (2002): Dysmyelination revealed through MRI as increased radial (but unchanged axial) diffusion of water. Neuroimage 17:1429–1436.

Sripada K, Løhaugen GC, Eikenes L, Bjørlykke KM, Håberg AK, Skranes J, Rimol LM (2015): Visual-motor deficits relate to altered gray and white matter in young adults born preterm with very low birth weight. Neuroimage 109:493–504.

Staudt M, Pavlova M, Böhm S, Grodd W, Krägeloh-Mann I (2003): Pyramidal tract damage correlates with motor dysfunction in bilateral periventricular leukomalacia (PVL). Neuropediatrics 34:182–188.

Stott DH, Moyes FA, Henderson SE (1984): Henderson revision of the Stott-Moyes-Henderson Test of Motor Impairment. Ontario: Brook Educational Publishing Ltd.

Tournier J-D, Mori S, Leemans A (2011): Diffusion tensor imaging and beyond. Magn Reson Med 65:1532–1556.

Volpe JJ (2009a): Brain injury in premature infants: a complex amalgam of destructive and developmental disturbances. Lancet Neurol 8:110–124.

Volpe JJ (2009b): The encephalopathy of prematurity--brain injury and impaired brain development inextricably intertwined. Semin Pediatr Neurol 16:167–178.

Wolke D, Meyer R (1999): Cognitive status, language attainment, and prereading skills of 6-year-old very preterm children and their peers: the Bavarian Longitudinal Study. Dev Med Child Neurol 41:94–109.

Figure legends

Figure 1. Probabilistic tractography. Differences in diffusion parameters (FA, AD, RD and MD) - between VP/VLBW and control adults in the probabilistically tracked whole CST (a) and along the z-axis of the CST (b). Approximate levels of the brain stem (BS), capsula interna (CI), corona radiata (CR) and centrum semiovale (CSO) are marked along the CST. Significant differences $p<0.05$ are marked with asterisk; for comparisons along the z-axis Bonferroni correction for multiple comparisons was used. Left and right CST are averaged.

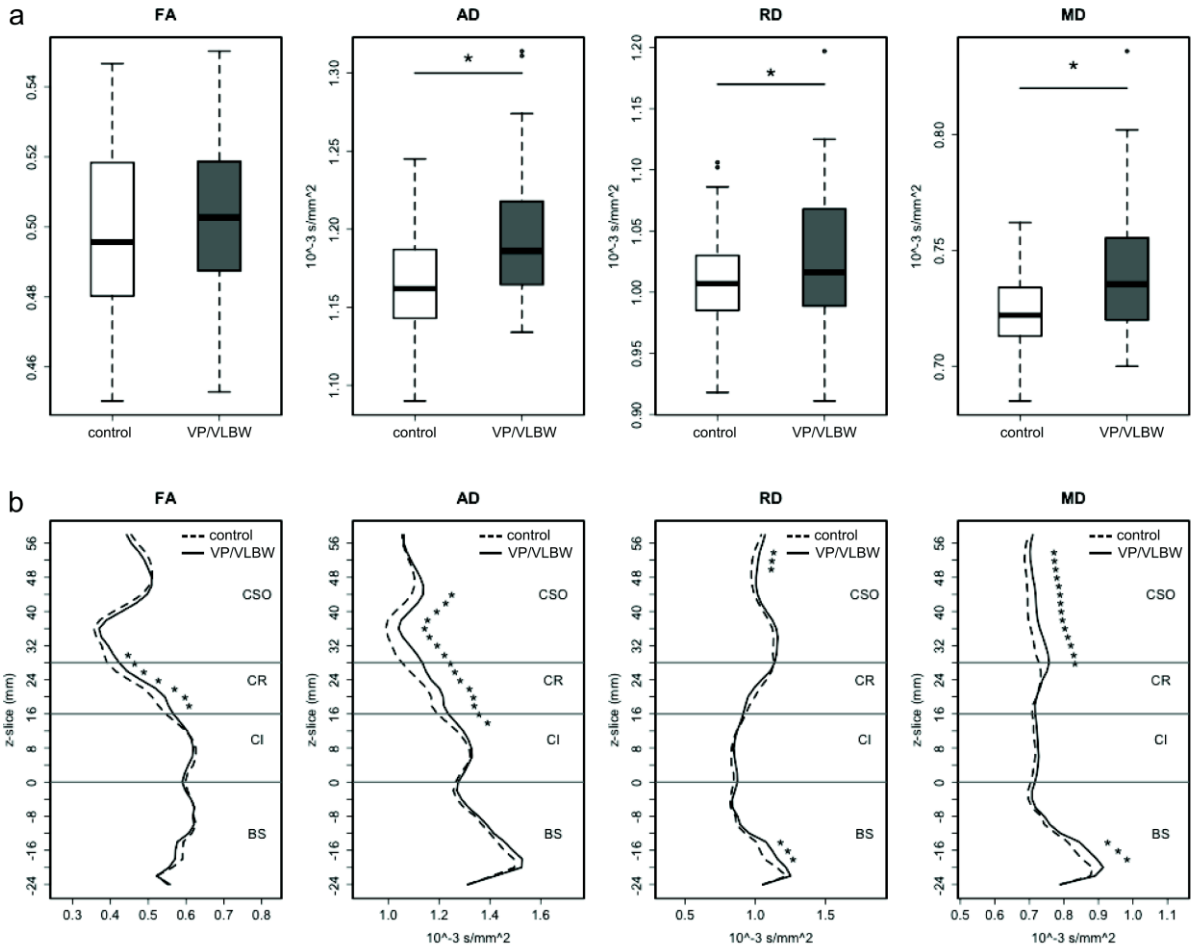

Figure 2. TBSS in the CST and right and left CST profiles (probabilistic tracking). Differences in diffusion parameters (FA, AD, RD and MD) between VP/VLBW and adult controls. Comparisons in the CST (in yellow) after TBSS and slice wise along the z-axis of the CST after probabilistic tracking. The significant TBSS skeleton voxels ($p<0.05$, with threshold-free cluster enhancement correction) along the CST are overlaid onto the MNI template brain. On the right and left of each brain, the slice wise CST profiles resulting from probabilistic tractography are depicted for each diffusion parameter and significant differences (Bonferroni corrected for multiple comparisons) are marked with asterisk.

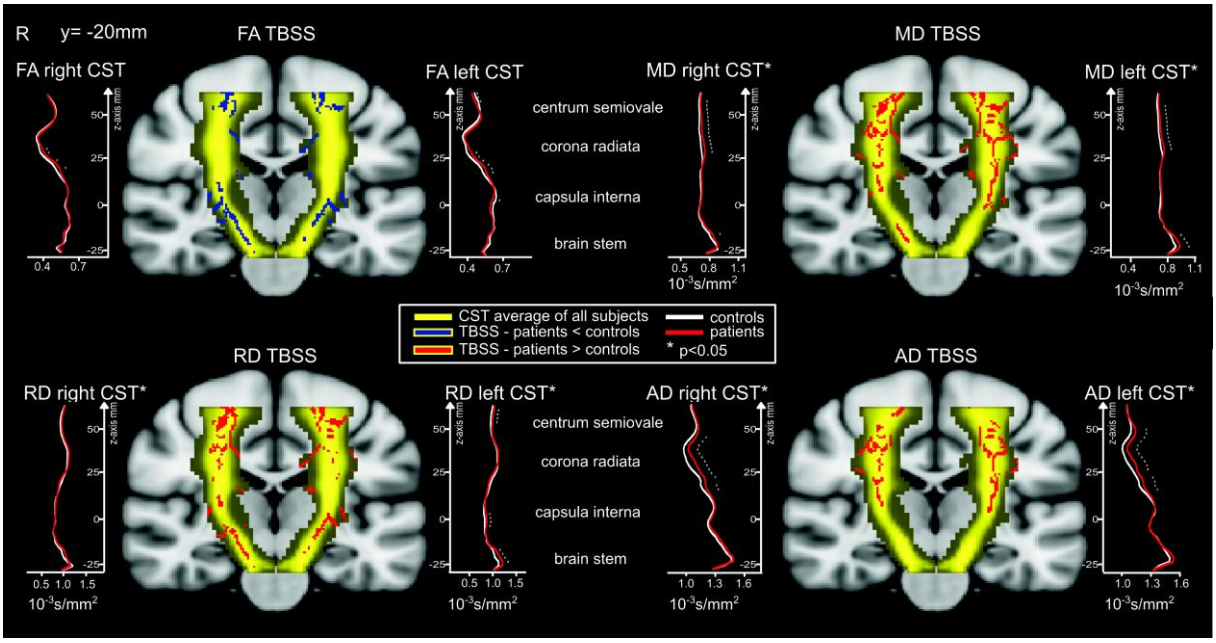

Figure 3. FLAIR MR images in six subjects - three control subjects (a,b,c) and three VP/VLBW subjects (d, e, f). Left panel (a, d) shows subjects without white matter hyperintensities while mid and right panels show subjects with white matter intentisities (arrows) along the corticospinal tract (b, e) or outside it (c, f). The CST is marked with a black outline.

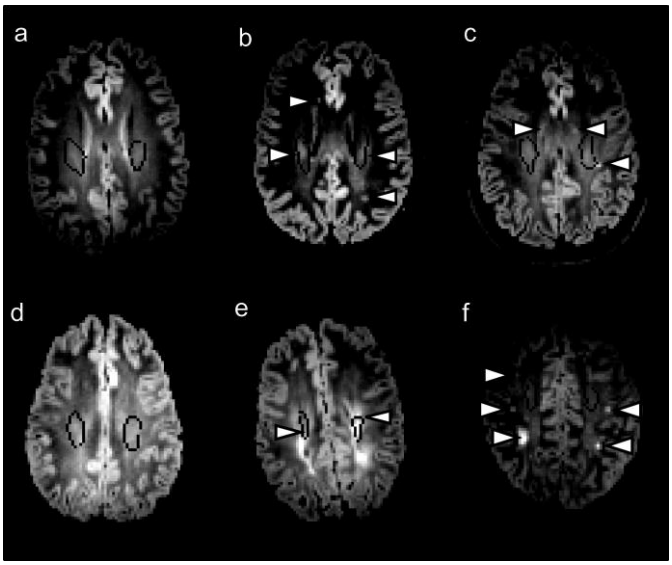

Figure Supplemental. Volumes of corpus callosum (at the midline level, of the interhemispheric cleft) and lateral ventricles in the control group (CON) and very preterm and/or low birth weight group (VP/VLBW). Volumes represent the white matter and corticospinal fluid segments resulting from SPM8 (http://www.fil.ion.ucl. ac.uk/spm) segmentation of the normalized T1-weighted images intersected with Juelich or Harvard atlas masks of corpus callosum respectively the lateral ventricles (from FSL www.fmrib.ox.ac.uk/fsl/). The six representative subjects from Figure 3 (a-c control subjects, d-f VP/VLBW subjects) are exemplified as normalized T1-w images (linearly coregistered to Montreal Neurological Institute standard space) and their respective volumes are marked as filled circles and a-f labels in the boxplots. In the T1-w images, (e) shows an obvious thinning of the corpus callosum and the black arrows in (d) and (e) show enlarged ventricles. The black horizontal line in the plots depicts one standard deviation below respectively above the mean of the control subjects.

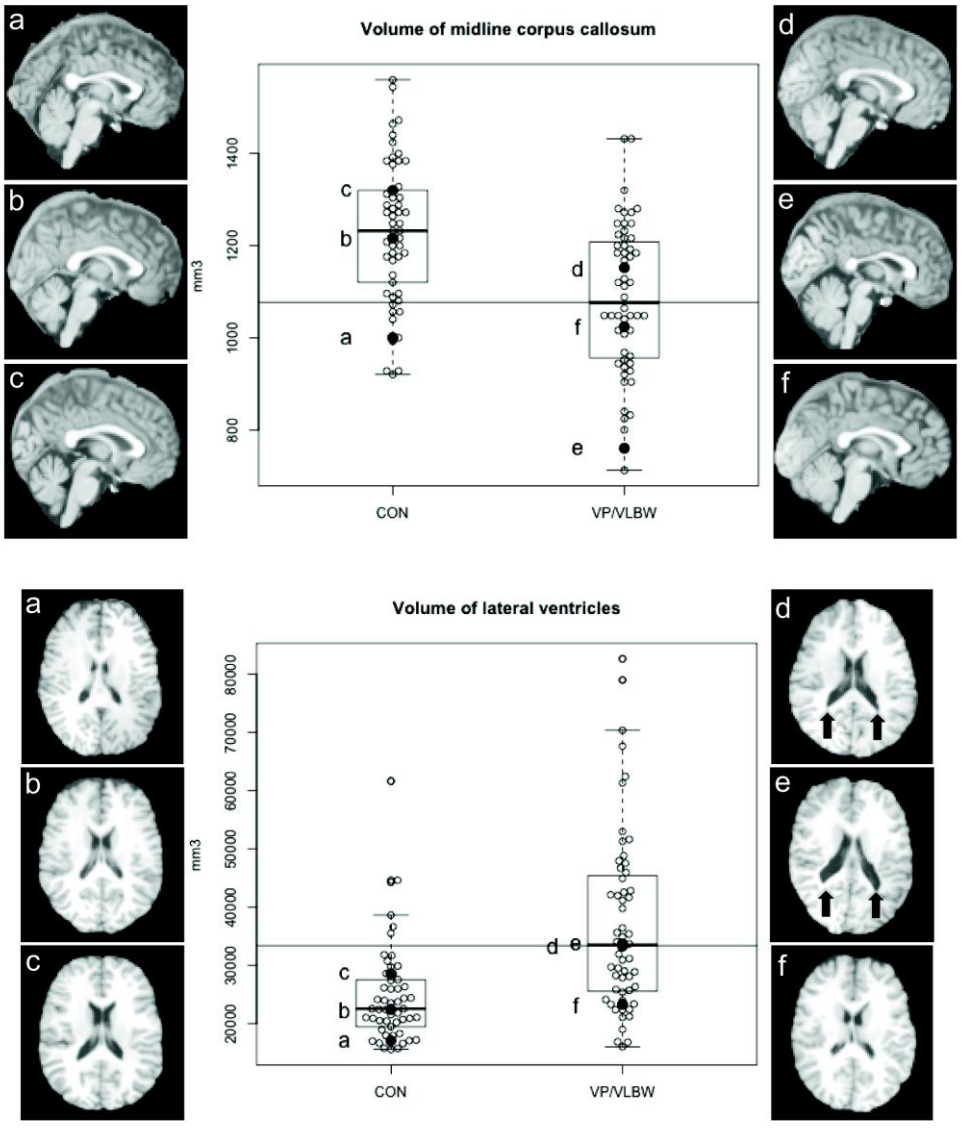

Tables

Table 1. Birth and scanner related measures (mean (standard deviation)) for the subjects included in the study, by group. Group differences were tested with a chi-squared test (gender and MRI site) or an independent samples t-test (age, gestational age, and birth weight).

	All controls n=53	All VP/VLBW n=56	p-value
Age, years	27.09 (0.79)	26.89 (0.6)	0.154
Sex, f/m	17/36	20/36	0.843
Gestational age at birth, weeks	39.64 (1.06)	30.38 (1.86)	<0.001*
Birth weight, grams	3336 (482)	1335 (316)	<0.001*
Optimality score	0.42 (0.69)	9.16 (2.53)	<0.001*
MRI site (n)			
Bonn:Achieva	8	3	0.132
Bonn Ingenia	10	27	0.005
Munich Achieva	19	23	0.537
Munich Ingenia	16	3	0.003

Table 2. Results of group comparisons (t-test) for the DTI parameters of probabilistically tracked CST. Significant differences p<0.05 are marked with asterisk.

	All controls n=53	All VP/VLBW n=56	p-value
FA	0.498(0.023)	0.503(0.021)	0.256
AD (10^{-3}s/mm^2)	1.162(0.035)	1.193(0.042)	<0.001*
RD (10^{-3}s/mm^2)	1.006(0.042)	1.027(0.054)	0.024*
MD (10^{-3}s/mm^2)	0.723(0.018)	0.740(0.028)	<0.001*

Table 3. Analysis of variance with CST white matter lesions as grouping variable (groups 1 to 4). When the overall ANOVA indicated a significant effect, *post hoc* comparisons (all combinations of subgroups) using the Tukey HSD test have also been performed. The *post hoc* contrasts 1-3 and 1-4 denote the difference between control subjects without visible CST lesions and VP/VLBW without (1-3), respectively VP/VLBW with CST lesions (1-4). Contrast 3-4 shows the influence of CST lesions within the VP/VLBW group. Mean (standard deviation) are also provided and significant differences are marked with asterisk.

	Controls 1. Without CST lesions n=50	Controls 2. With CST lesions n=3	VP/VLBW 3. Without CST lesions n=38	VP/VLBW 4. With CST lesions n=18	ANOVA
Age, years	27.09(0.78)	27.11(1.07)	26.91(0.58)	26.86(0.67)	F(3,105)=0.7071,p=0.5499
Gestational age at birth, weeks	37.67(1.15)	30.17(1.89)	39.76(0.94)	30.47(1.87)	F(3,105)=349.1,p<0.001* 1-2: p=0.09 1-3: p<0.001* 1-4: p<0.001* 2-3: p<0.001* 2-4: p<0.001* 3-4: p=0.891
Birth weight, grams	3356 (473)	3007 (627)	1321(311)	1363 (331)	F(3,105)=222.9,p<0.001* 1-2: p=0.47 1-3: p<0.001* 1-4: p<0.001* 2-3: p<0.001* 2-4: p<0.001* 3-4: p=0.98
FA	0.50 (0.02)	0.50 (0.05)	0.50 (0.02)	0.51 (0.02)	F(3,105)=0.6359,p=0.593
AD (10^{-3}s/mm^2)	1.16 (0.03)	1.19 (0.05)	1.19 (0.03)	1.21 (0.05)	F(3,105)=8.688,p<0.001 1-2: p=0.689 1-3: p=0.017* 1-4: p<0.001* 2-3: p=1

					2-4: p=0.688 3-4: p=0.077
MD (10^{-3}s/mm^2)	0.72 (0.02)	0.74 (0.02)	0.74 (0.02)	0.75 (0.03)	F(3,105)=6.839,p<0.001* 1-2: p=0.756 1-3: p=0.032* 1-4: p<0.001* 2-3: p=1 2-4: p=0.778 3-4: p=0.182
RD (10^{-3}s/mm^2)	1.00 (0.04)	1.02 (0.07)	1.02 (0.05)	1.04 (0.07)	F(3,105)=2.23,p=0.089